Optics and Lasers in Engineering 20 (1994) 241–257

0143-8166/94/$07·00

Variable Sensitivity Moiré Interferometry Using Binary Optic Technology†

Helen Johnson-Cole,[a]* John A. Gilbert[b] & James H. Bennewitz[c]

[a]NASA Marshall Space Flight Center, Huntsville, Alabama 35812, USA
[b]University of Alabama in Huntsville, Huntsville, Alabama 35899, USA
[c]AT&T Bell Laboratories, Allentown, Pennsylvania 18103, USA

ABSTRACT

This paper demonstrates the feasibility of optical microlithography as a grating production method for use in variable sensitivity moiré interferometry. In this study, a crossed, binary, phase-type grating is produced and replicated onto the surface of the test piece. Moiré interferograms are recorded with sensitivities ranging from 2.0 *to* 0.40 *μm/fringe. Generalized expressions are given for variable sensitivity moiré interferometry, and experimental tests are conducted to verify analytical arguments. In one of these tests, two different diffraction order pairs are used simultaneously to verify that surface displacement can be measured at different sensitivities.*

INTRODUCTION

In 1965, Dally and Riley[1] wrote: 'If and when higher quality line arrays with line spacings of 10,000 to 30,000 lines/in. become available, the moiré method may see more general usage in a wider range of experimental stress analysis.' That level of technical sophistication was met when Post proposed an approach to in-plane surface displacement measurement called moiré interferometry.[2] The method involves the transfer of a reflective, linear phase-type grating (of frequency up to

† Portions of this manuscript were presented at the Society for Experimental Mechanics' Spring Conference on Experimental Mechanics, Milwaukee, Wisconsin, 9–12 June 1991.

* To whom correspondence should be addressed.

2,000 lines/mm or 50800 lines/in.) from an interferometrically generated mold to an actual prototype.[3] The technique has rapidly grown in popularity since its introduction in 1980 because it offers very high sensitivity, excellent contrast and good spatial resolution.[4]

In conventional moiré interferometry, a reflective phase-type sinusoidal grating is generated interferometrically and transferred to a specimen. The sinusoidal grating diffracts practically no light into the harmonic orders greater than 1, and only the -1 and $+1$ diffraction orders can be combined to create an interferometric fringe pattern. In this case, the sensitivity is fixed at half the pitch of the specimen grating. This fixed sensitivity requires that the investigator should have some prior knowledge of the magnitude of the displacement to be studied, and places restrictions on the examination of regions in which high strain gradients occur. To overcome this experimental difficulty, Wang and his colleagues developed a composite grating with two different grating frequencies.[5] The grating was generated interferometrically and transferred to a single-edge notched specimen. The specimen was loaded to failure to estimate the J-integral value.

This paper presents an alternative method for achieving variable sensitivity moiré interferometry. The approach relies on a new technology called binary optics, first introduced into the literature in the late 1980s.[6,7] This technology is based on the use of state-of-the-art optical microlithography processes to pattern and etch the surface of an optical substrate or a silicon wafer with extreme precision and detail.[8] In this study, an etched silicon wafer is used as a mold for replicating and transferring a reflective diffraction grating to a specimen surface. The wafer was produced in 1988 at AT&T Bell Laboratories to test the capabilities of a new step and repeat system. The square wave profile etched on the wafer was subsequently identified by the authors as a feasible candidate for implementing variable sensitivity moiré interferometry as described herein. The surface characterization of the etched wafer is discussed and experiments are performed in which surface displacements are measured using different diffraction order pairs.

ANALYSIS

In variable sensitivity moiré interferometry a silicon wafer mold is produced so that a grating can be transferred to a specimen. The specimen is symmetrically illuminated with coherent light at angles α_m

such that the +m and −m diffraction orders propagate collinearly along a path normal to the grating surface. The illuminating beams produce a virtual grating on the surface having a spatial frequency, f_v, given by

$$f_v = \frac{2 \sin (\alpha_m)}{\lambda} \tag{1}$$

where λ is the wavelength of the illuminating source. When the specimen is loaded, the diffracted wavefronts interfere to produce a pattern which can be described in terms of the conventional moiré equation

$$U = Np \tag{2}$$

where N is the fringe order number and p is the pitch of the reference grating ($1/f_v$). In the case of variable sensitivity moiré interferometry, the spatial frequency of the virtual grating is $2m$ times that of the fundamental frequency, f, of the specimen grating. Therefore, the displacement measured perpendicular to the lines in the reference grating is given by

$$U = \frac{N}{f_v} = \frac{N}{2mf} \tag{3}$$

Equations (1)–(3) show that in-plane displacement is measured with a sensitivity that depends on the pitch of the specimen grating and the diffraction order pair being used. To achieve variable sensitivity, a high-quality grating is required which has a symmetric profile sufficient to diffract a usable amount of light into a variety of orders. This paper demonstrates that the method of optical microlithography can be used to create such a grating.

OPTICAL MICROLITHOGRAPHY

Improved techniques in microlithography and advancements in step and repeat systems (wafer steppers) are now meeting the requirements for submicron design rules in the electronics industry and, more recently, in the optics industry. This progress has been driven by many factors including improvements in lens design and fabrication, refinements in

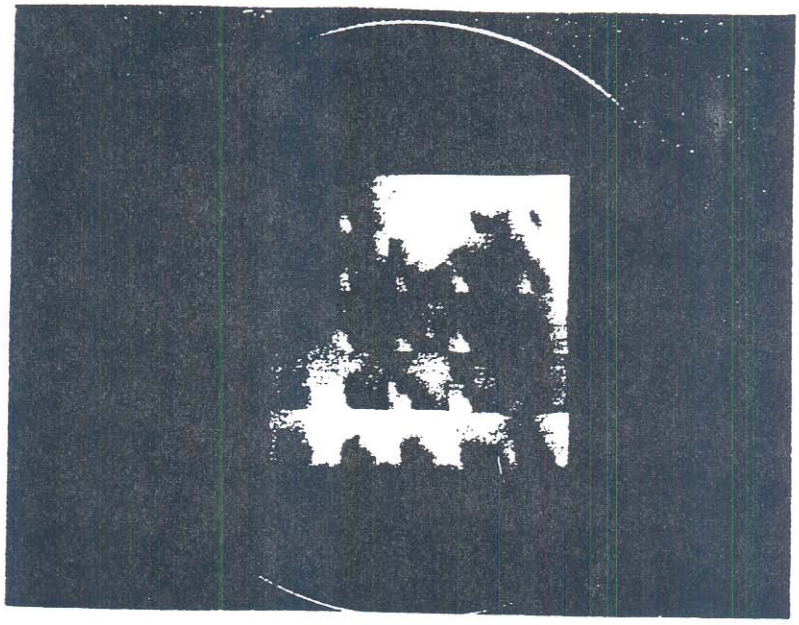

Fig. 1. Photograph of a silicon wafer with a crossed, square wave grating.

optical resists, and the ability to retrofit innovations into existing machines. Past projections by one of the authors indicated that optical microlithography could eventually be used to produce integrated circuit devices with less than 0.5 μ design rules.[9] This is now the case.

AT&T Bell Laboratories has developed a deep UV step and repeat system capable of achieving 0.5 μm resolution within a 14.5 mm field under routine use, and even higher resolution (0.35 μm) under more limited conditions. An earlier paper by the present authors and their collaborators[10] suggested that optical microlithography could be applied to produce a master grating of continuous pitch for use in moiré interferometry. Figure 1 shows a silicon wafer manufactured in conjunction with testing the step and repeat system and subsequently used in the present study. This wafer contains a crossed square wave grating pattern that covers a total of 25 cm^2 of the wafer surface. The pattern is composed of an array of individual squares that each contain an identical crossed square wave grating pattern. The individual square patterned areas are created one at a time, and each square is very closely matched at its boundary with the adjacent squares using a step and repeat scheme. The segmentation of the overall grating is due to limitations on the field size that could be produced with the system at the time.

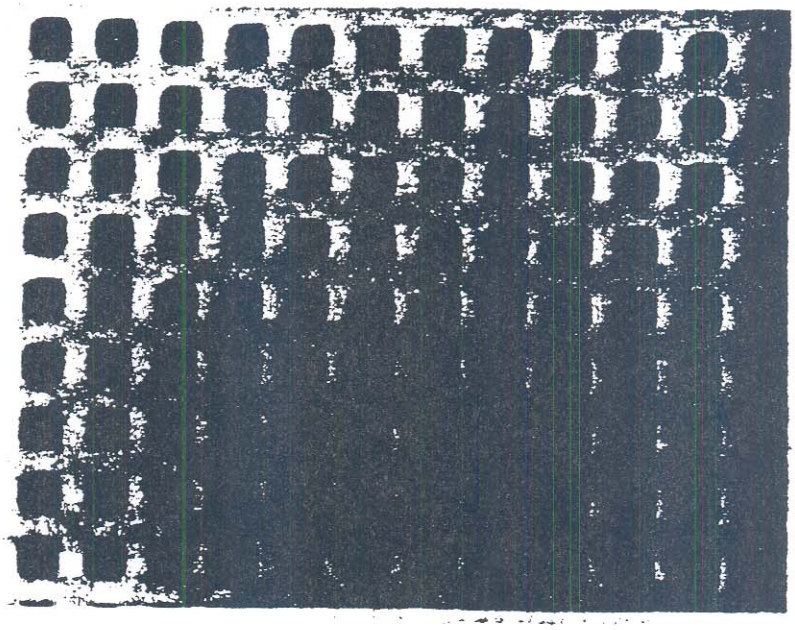

Fig. 2. Microscopic image of the silicon wafer with a crossed, square wave grating (×691).

SURFACE CHARACTERIZATION

A Nomarski microscope was used to verify the orientation and pitch of the pattern etched on the silicon wafer shown in Fig. 1. The photograph, shown in Fig. 2 and originally taken with a magnification of 691, demonstrates that the grating has a two-dimensional, crossed square wave profile. The pitch of the grating is 4.0 μm and the widths of the crest and trough are both equal to 2.0 μm.

Further characterization of the crossed grating wafer using a scanning electron microscope measured the height of the grating at 0.5 μm, and verified that the profile was extremely close to the expected square wave shape. Even though the square wave grating has a frequency of 250 lines/mm, which is significantly lower than the frequency of the interferometric gratings used in conventional moiré interferometry (typically 1200–2000 lines/mm), the profile diffracts a number of harmonics which allow displacement to be measured over an extended range.

Equations (1) and (3) predict that as many as seven diffraction order

TABLE 1
Range of Sensitivity

Angle of illumination, α_m *(deg)*	*Diffraction order pair, m*	*Sensitivity,* p_v
7·4	1	2 μm/fringe
14·9	2	1 μm/fringe
22·7	3	0·666 μm/fringe
31·0	4	0·500 μm/fringe
40·0	5	0·400 μm/fringe
50·0	6	0·333 μm/fringe
64·2	7	0·285 μm/fringe

pairs may be used for displacement analysis when this square wave grating is illuminated with a wavelength of 514.5 nm. Table 1 lists the seven diffraction order pairs along with the required angle of illumination and resulting sensitivity associated with each possible combination. Provided that light is efficiently diffracted into the appropriate orders, the potential sensitivity range for this grating extends from 2.0 μm/fringe (corresponding to a virtual grating of 500 lines/mm) to 0.285 μm/fringe (corresponding to a virtual grating of 3500 lines/mm). The lower sensitivity limit on this range is directly related to the frequency of the specimen grating, and the upper limit on sensitivity is theoretically never greater than 0.25 μm/fringe.[11] From a practical standpoint, however, the upper sensitivity limit in variable sensitivity moiré interferometry is really a function of the grating profile and its associated diffraction efficiency.

When a scalar diffraction theory approach was applied to the grating profile, diffraction efficiencies were found to be in the neighborhood of 0.1%. This low diffraction efficiency can be attributed to the fact that the simple geometry chosen for system testing by AT&T was developed independently from the current investigation and therefore was not optimized for diffraction efficiency. In fact, over 97% of the light incident on the grating is directly reflected into the zeroth order; consequently, only 3% of the incident light is diffracted by the remaining harmonics. The relative intensity of the even diffraction orders is diminished because the grating profile has a crest equal to half the pitch. However, a modified profile has been designed for increased diffraction efficiency and is currently under production. Nonetheless, the wafer shown in Fig. 1 performs sufficiently well to demonstrate clearly the technique of variable sensitivity moiré interferometry as described in the following section.

VARIABLE SENSITIVITY EXPERIMENTS AND RESULTS

Two experiments were performed to demonstrate the variable sensitivity method. The first experiment combines the third order diffraction pair and uses the carrier fringe/double exposure technique to study the fringe field that results from a known loading state. The second experiment demonstrates that the third- and fifth-order diffraction pairs can be used simultaneously to measure displacement at different sensitivities. Both of these experiments require that a grating be transferred from the silicon wafer to the test surface. The transfer process is discussed next, after which the experiments are described.

A very weak solution of Kodak Photoflow in deionized water was spun onto several bare crossed grating wafers before coating them with aluminum. The wafers were allowed to spin until fairly dry. Next they were placed in a desiccative environment and, when thoroughly dry, overcoated with aluminum. For this process, the wafers were placed in a planetary vacuum deposition chamber and overcoated with a layer of aluminum, approximately 300 nm thick. They were slowly rotated during deposition to insure even coating of the walls of the grating.

A thin coat of epoxy was initially applied to the notched beam shown in Fig. 3, and the epoxied surface was placed face down on the aluminized wafer. The edges of the specimen were carefully aligned with the cross grating to provide a means for measuring displacement components along X and Y. After the epoxy cured, the specimen was

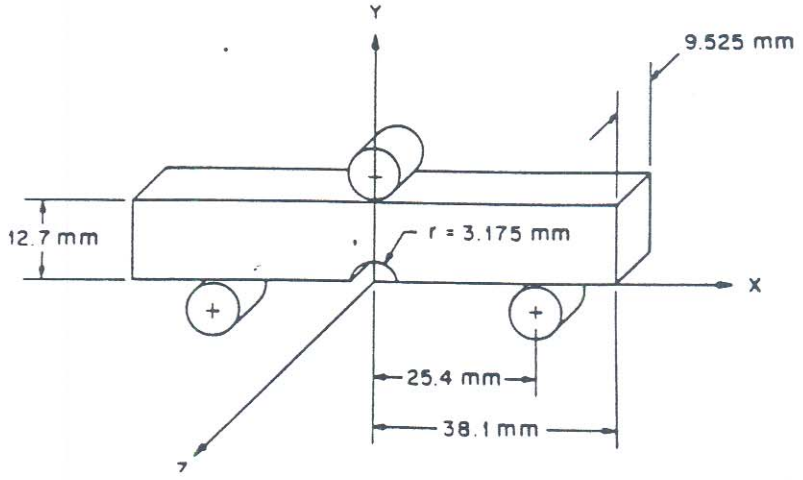

Fig. 3. Dimensions of circularly notched beam specimen.

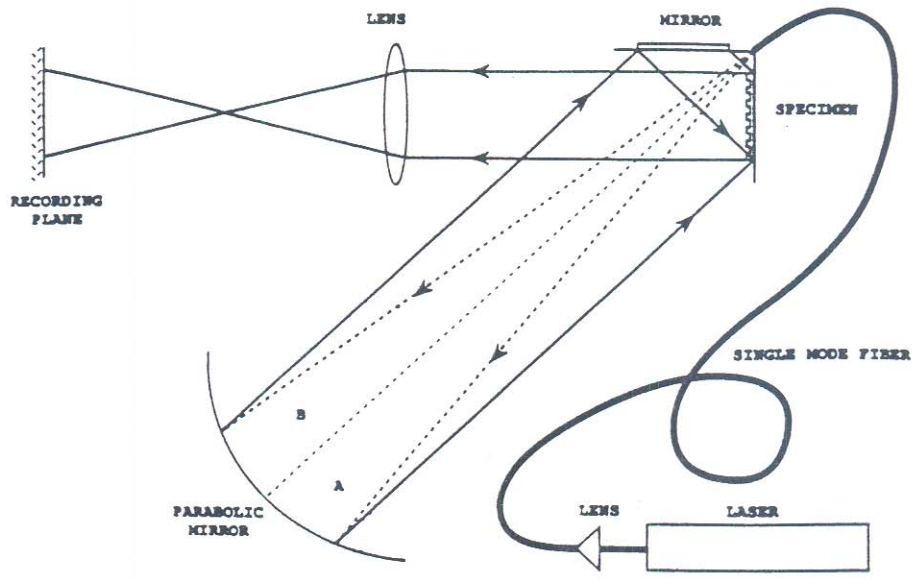

Fig. 4. Experimental set-up for moiré interferometry.

pried loose taking great care not to break the wafer. Excess epoxy was removed.

Figure 4 shows the experimental set-up used to record interferometric moiré patterns with variable sensitivity from a grating deposited on the surface of the notched beam. An unexpanded argon ion laser beam of 514.5-nm wavelength was launched into a single mode step index fiber using a 5× microscope objective. The exit end of the fiber was placed at the focal point of an on-axis parabolic mirror (2 m focal length, 0.41 m diameter), thereby producing a collimated beam with Gaussian intensity distribution. The parabolic mirror reflected the collimated light back to the specimen-holder assembly where a flat mirror was positioned at 90° to the specimen. Rotation of the entire assembly about a vertical axis centered at the focal point of the parabolic mirror controlled the angle of illumination. Figure 4 illustrates that the stage may be adjusted so that the diffraction order produced by the direct beam A coincides with that produced by the reflected beam B. In this case, both wavefronts are diffracted along the normal to the specimen surface and pass through a 38.1-mm diameter, 375-mm focal length imaging lens. The notched beam was placed in three-point bending and the stage was oriented to illuminate the specimen symmetrically at an angle of 22.7° with respect to its normal. This illumination angle corresponds to the third diffraction order pair;

Table 1 shows that displacement is measured at a sensitivity of 0.666 μm/fringe.

As the longitudinal axis of the notched beam was oriented parallel to the lines in the interference zone of the two illuminating plane waves, the displacement component measured was perpendicular to its longitudinal axis. A carrier pattern, or linear phase shift between the two diffracted wavefronts, was introduced by rotating the specimen in the plane of the specimen grating. The initial pattern, corresponding to the pre-load condition, was photographed in the image plane and is shown in Fig. 5(a). Figure 5(b) shows a photograph of the modulated carrier pattern after the two rollers supporting the beam were displaced 0.0038 mm (0.00015 in.) in the positive Y direction, relative to the fixed central roller. A double exposure of the initial carrier pattern superimposed

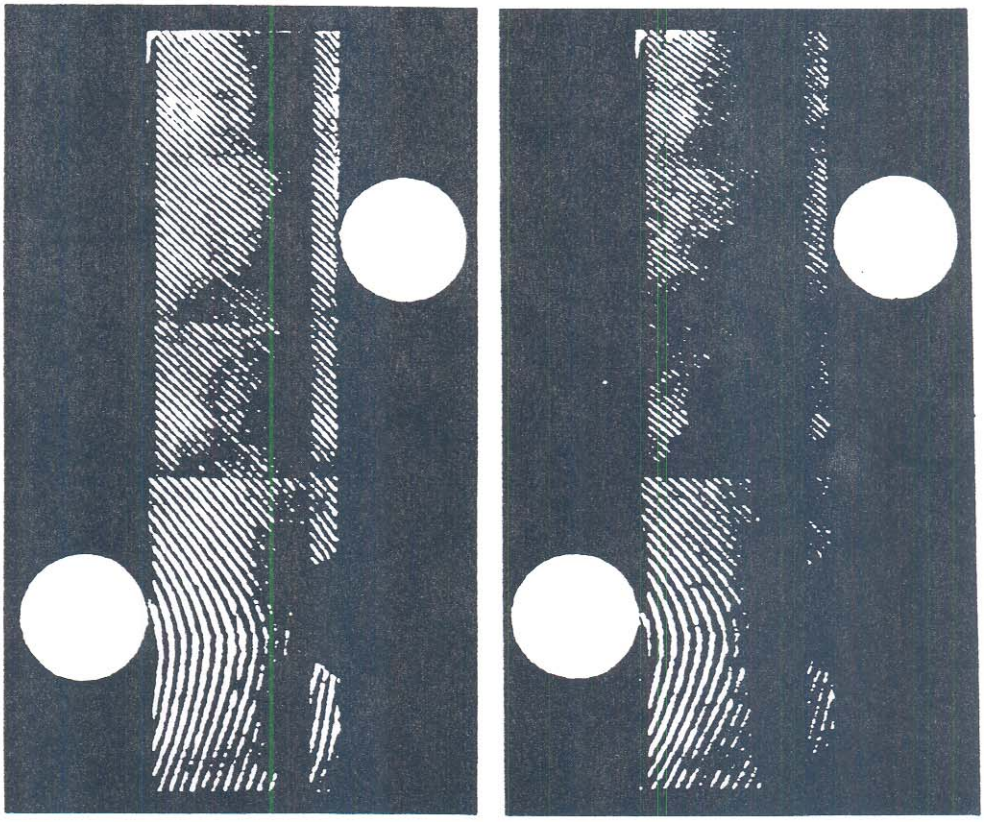

Fig. 5. The V displacement field: (a) initial carrier pattern, (b) modulated carrier pattern.

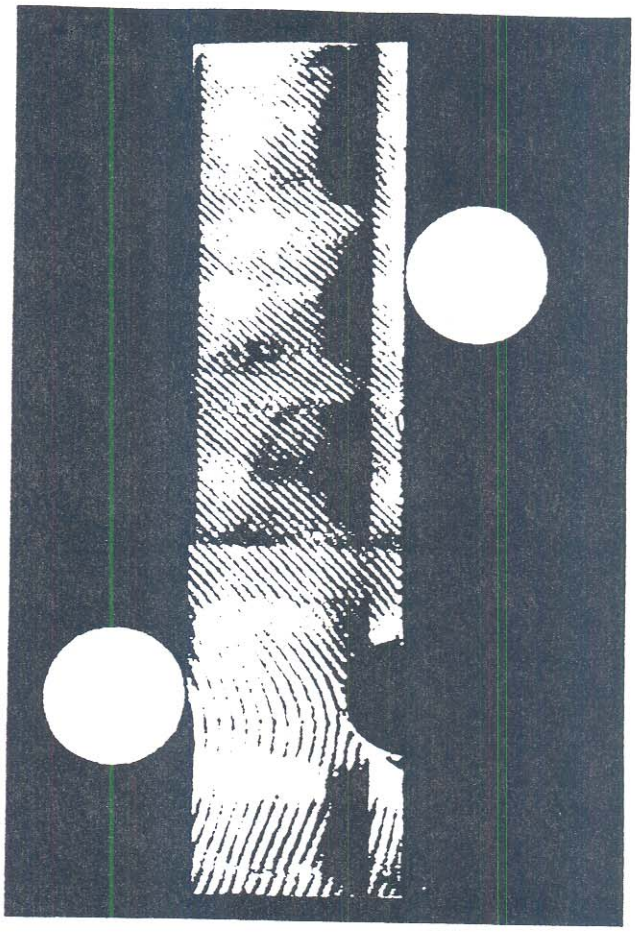

Fig. 6. Double exposure of the initial and modulated carrier patterns for the V displacement field.

with the modulated carrier pattern is shown in Fig. 6. The moiré fringe pattern represents the full-field in-plane displacement field along the transverse direction of the specimen. As this component is measured along the y-axis, it is referred to as the V displacement field. Numbers may be assigned to the moiré fringes starting with zero at the center support; consequently, the fringe order number at the outer support is 5.5. Equation (1) establishes the pitch of the virtual grating, p_v, at 1/1500 mm. Using Eqn 3, the transverse displacement component, V, at the outer beam support is calculated at 0.0037 mm. The interferometrically measured displacement agreed closely with the imposed value of 0.0038 mm.

The experiment described above was repeated to determine the U displacement field along the longitudinal axis of the notched beam. The beam was oriented with its longitudinal axis perpendicular to the lines in the interference zone of the two illuminating wavefronts, and the same procedure as described above was applied. (As opposed to rotating the specimen and repeating the experiment, the U and V displacement patterns could have been recorded simultaneously by symmetrically illuminating the specimen in two perpendicular directions.) Figure 7 shows a double exposure of the carrier pattern in its initial and modulated states. The moiré fringes may be numbered

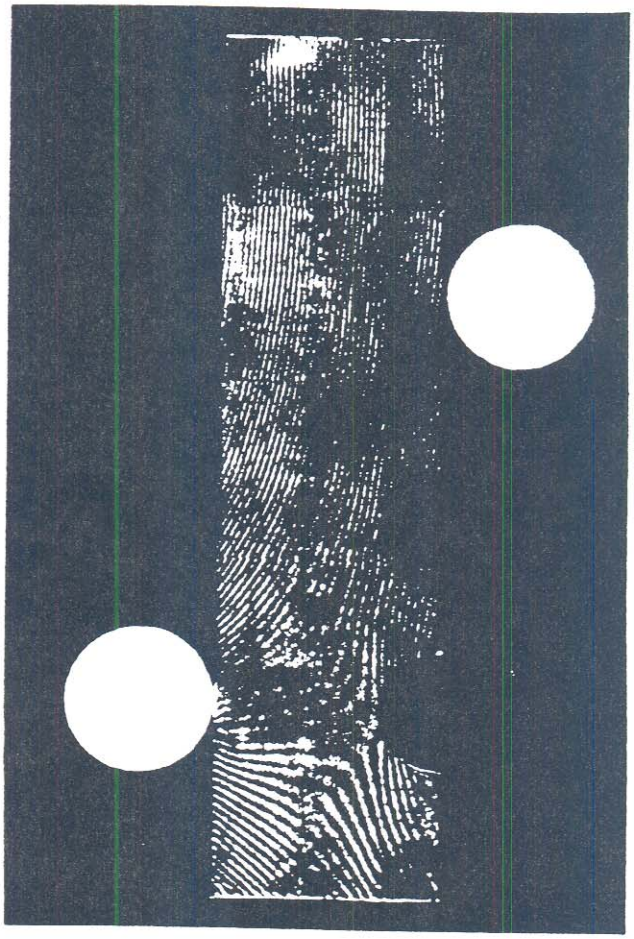

Fig. 7. Double exposure of the initial and modulated carrier patterns for the U displacement field.

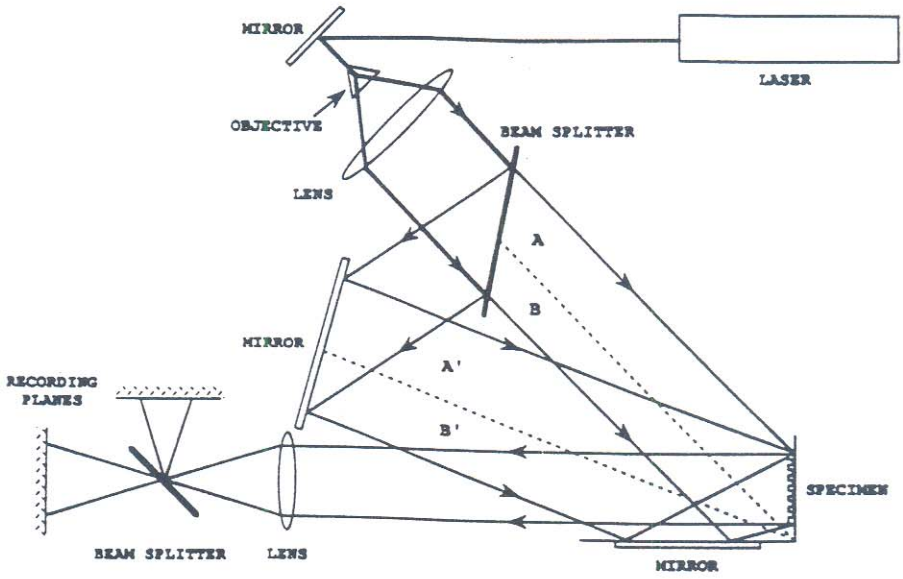

Fig. 8. Experimental set-up for simultaneously recording displacement at two different sensitivities.

starting with zero at the center support. Equation (3) can be used to obtain the U displacement.

A second experiment was conducted to demonstrate that moiré patterns having different sensitivity could be recorded simultaneously. Figure 8 shows an argon ion laser beam expanded by a spatial filter and collimated using a lens. The collimated beam was directed to the specimen holder assembly where it illuminated the specimen and a flat mirror positioned at 90° to the specimen surface. The specimen holder assembly was rotated about a vertical axis and positioned such that the propagation vector of the illuminating beam made a 40° angle with respect to the specimen grating normal. This orientation was chosen to create a virtual grating (formed in space as a result of the interference of the direct beam, A, and the reflected beam, B) having a spatial frequency 10 times that of the specimen grating. A beam splitter was placed in the collimated illuminating beam and the split beam was directed at the specimen holder assembly using an adjustable flat mirror. The propagation direction of the collimated split beam was chosen to interrogate the specimen with a virtual grating having a frequency six times that of the real grating. When appropriately illuminated, the -3 and $+3$ diffraction orders from beams A′ and B′, respectively, were collinearly diffracted together with the -5 and $+5$

diffraction orders from beams A and B. In this case, four wavefronts were simultaneously diffracted from the specimen surface along the grating normal!

The notched specimen was placed in a three point bending frame and the frame was oriented such that the longitudinal axis of the beam was parallel to the lines in the interference zone of the two illuminating wavefronts. This orientation allowed the displacement component perpendicular to the longitudinal axis of the beam to be measured. The optical system was fine-tuned to achieve an initial interference pattern for each of the diffraction order pairs being used. This was accomplished by first blocking illuminating beams A and B to produce an initial pattern with the third-order diffraction pair, then by blocking beams A′ and B′ and unblocking beams A and B to yield an initial interference pattern with the fifth-order diffraction pair. A vertical carrier pattern was generated by rotating the loading frame assembly about a vertical axis.

The double exposure method was used to study and compare the response of the third-order pair and fifth-order pair to an identical loading condition. A beam splitter was placed behind a single imaging lens, as shown in Fig. 8, to make this comparison possible. A Polaroid camera back was positioned in each of the two image planes of the recording system. Beams A and B were blocked and an initial carrier pattern, produced by the third order diffraction pair, was photographed in recording plane 1. The film positioned in recording plane 1 remained undisturbed. Then beams A and B were unblocked and beams A′ and B′ were blocked. The film in recording plane 2 was then exposed to an initial carrier pattern produced by the fifth-order pair. Next, the model was loaded by displacing the two rollers supporting the notched beam in the positive Y direction. The film in recording plane 2 was exposed to the fifth order diffraction pair for a second time, but this time it was exposed to a modulated carrier pattern corresponding to the load-induced condition of the model. Finally, beams A′ and B′ were unblocked and beams A and B were blocked and the previously exposed film in recording plane 1 was exposed to the modulated carrier pattern produced by the third-order diffraction pair. Figure 9 shows a double-exposure recording of the initial and modulated carrier patterns produced by the third diffraction order pair. Similarly, Fig. 10 shows the double-exposure moiré interferometry recording that was produced using the fifth order pair. The patterns are transposed due to the reflection at the splitter. Moiré fringe order numbers were assigned in both figures starting with zero at the center support above the notch.

A comparison of Figs 9 and 10 verifies Eqn 3, and illustrates that the

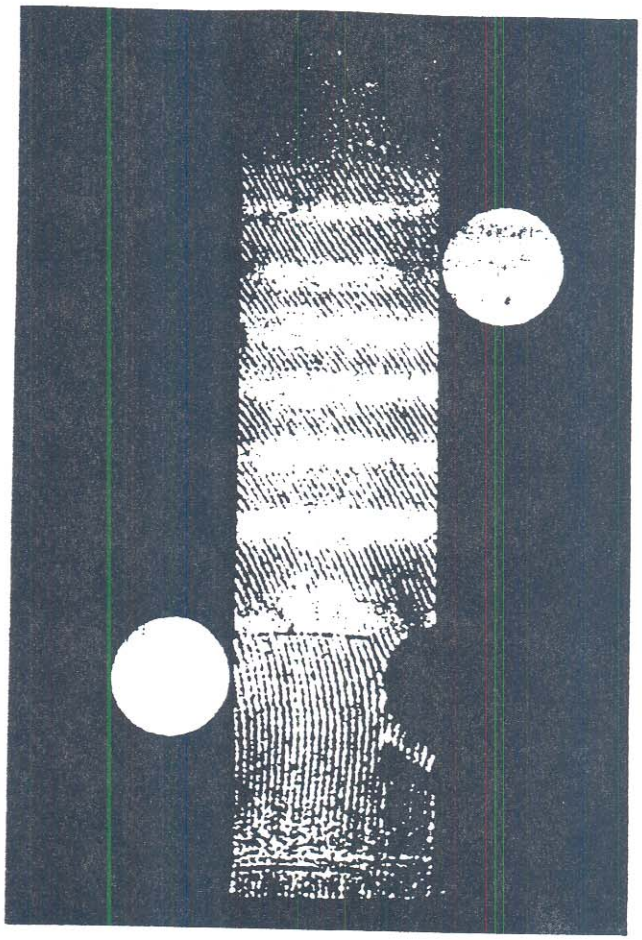

Fig. 9. Interferometric moiré pattern with sensitivity of 0.666 μm/fringe.

sensitivity is governed in part by the diffraction orders used. From Table 1, moiré fringes recorded using the third-order diffraction pair have a sensitivity of 0.666 μm/fringe whereas the sensitivity of measurement using the fifth-order diffraction pair is greater (it is equal to 0.400 μm/fringe). Equation (3) dictates that points contained within the fringe distribution shown in Fig. 10 should have a fringe order number that is 1.666 times the fringe order number of the corresponding point in Fig. 9. This can be verified quantitatively by considering the fringe order numbers at the outer roller support. In Fig. 9 the fringe order at this location is approximately 5.5, whereas the fringe order number at the corresponding point in Fig. 10 is approximately equal to 9.0, making the ratio roughly 1.6.

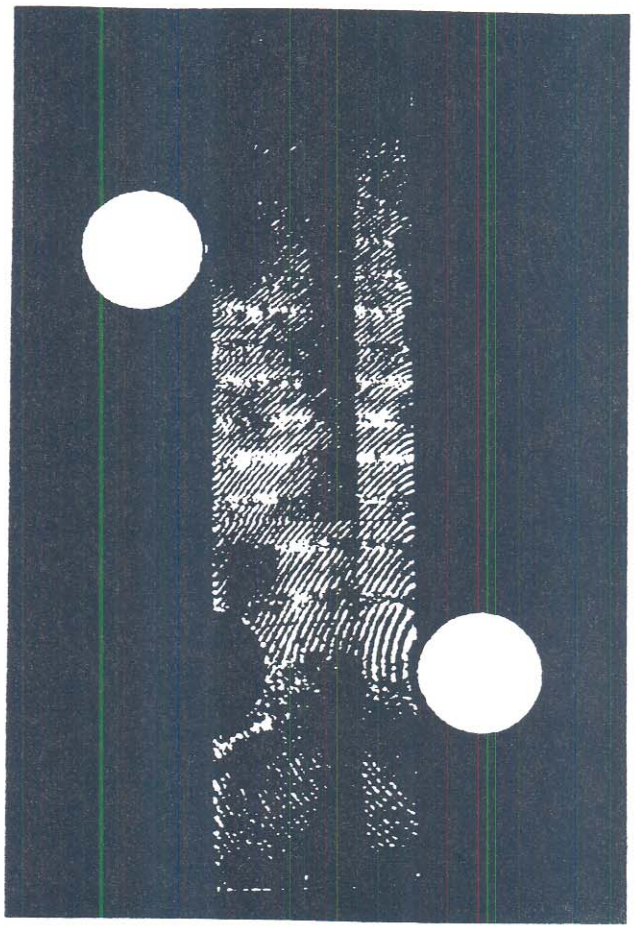

Fig. 10. Interferometric moiré pattern with sensitivity of 0.400 μm/fringe.

DISCUSSION

This paper has clearly demonstrated that a binary grating produced with optical lithography can be successfully applied to moiré interferometry for variable sensitivity measurement. The grating profile applied in this study exhibited diffraction efficiencies sufficient to demonstrate the technique, and moiré interferograms were recorded with exposure times of the order of a tenth of a second. Efforts are currently under way to design and produce grating profiles with multiple diffraction orders having higher and equal efficiencies. In the future, the profile could be shaped to facilitate coating of the wafer and transfer of the grating to the specimen; for example, by making the

profile triangular. In addition to creating profile shapes impossible to achieve interferometrically, optical microlithography could also be used to fabricate gratings with geometries specifically tailored to a particular application. For example, a set of equally spaced concentric circles could be produced to study radial displacements in the neighborhood of a crack tip. New replication techniques could be developed so that several submasters can be produced from a single silicon wafer. This would facilitate technology transfer and make the overall approach to moiré interferometry more economical.

CONCLUSION

Conventionally, the gratings used in moiré interferometry are created interferometrically and diffract all usable light into the -1 and $+1$ diffraction orders, thereby fixing the sensitivity of measurement at half the pitch of the specimen grating. An alternative approach to grating production was developed in this paper, where it was shown that optical microlithography could be used to manufacture a binary diffraction grating having a square wave profile. The grating diffracted light into multiple orders, and tests were conducted to show that different diffraction orders could be used to vary displacement sensitivity once the grating was transferred to the surface of a test specimen.

The work reported herein represents a unique contribution to the scientific community in the area of moiré interferometry. In light of recent advancements in the state of the art, researchers will soon be able to secure affordable, replicable, high-frequency, high-efficiency, customized gratings that have improved performance over conventional interferometric gratings. To this end, the authors have completed the design of grating profiles optimized for variable sensitivity moiré interferometry and are in the process of fabricating the corresponding binary optical elements. These developments will be reported in the near future.

ACKNOWLEDGEMENTS

The authors wish to express their thanks to Mr Curtis Bahr of MSFC/NASA for helping to coat the wafers, Dr Jean Bennett of China Lake Naval Weapons Research Laboratory for helping to characterize the profiles, and Dr Victor Pol of AT&T Bell Laboratories in Murray Hill, NJ, for helping with wafer production.

REFERENCES

1. Dally, J. W. & Riley, W. F., *Experimental Stress Analysis*, 1st edn. McGraw-Hill, New York, 1965, pp. 360–1.
2. Post, D., Moiré interferometry at VPI & SU. *Experimental Mechanics*, **23**(2) (1983) 203–10.
3. Post, D., Moiré interferometry. In *Handbook on Experimental Mechanics*, ed. A. L. Kobayashi. Prentice Hall, Englewood Cliffs, NJ, 1987, pp. 314–84.
4. Post, D., Moiré interferometry: advances and applications. In *Proc. 1990 Int. Conf. on Hologram Interferometry & Speckle Metrology*. The Society for Experimental Mechanics, 1990, pp. 1–13.
5. Wang, F., Kang, B. S.-J. & Kobayashi, A. S., Composite grating for moiré interferometry. *Optical Engineering*, **27**(7) (1988) 564–9.
6. Swanson, G. J., Binary optics technology: The theory and design of multi-level diffractive optical elements. MIT Technical Report 854, MIT Cambridge, MA, 1989.
7. Swanson, G. J., Binary optics technology: Theoretical limits on the diffraction efficiency of multilevel diffractive optical elements. MIT Technical Report 914, Cambridge, MA, 1991.
8. Pol, V., Bennewitz, J. H., Escher, G. C., Feldman, M., Firtion, V. A., Jewell, T. E., Wilcomb, B.E. & Clemens, J. T., Excimer laser-based lithography: A deep ultraviolet wafer stepper. In *Proc. SPIE Conf. on Optical Microlithography V*, Vol. 633. The International Society for Optical Engineering, 1986, pp. 6–16.
9. Bennewitz, J. H., Escher, G. C., Feldman, M., Firtion, V. A., Jewell, T. E., Pol, V., Wilcomb, B. E. & Clemens, J. T., Excimer laser-based lithography for 0.5 micron device technology. *Proc. IEEE/IEDM Conf.* The Institute of Electrical and Electronic Engineers, 1986, pp. 312–15.
10. Johnson, H. S., Gilbert, J. A., Dudderar, T. D., Bennewitz, J. H. & Matthys, D. R., New methods for recording and processing high frequency moiré patterns. *Proc. 1987 SEM Spring Conf. on Experimental Mechanics*. The Society for Experimental Mechanics, 1987, pp. 62–70.
11. Weissman, E. M. & Post, D., Moiré interferometry near the theoretical limit. *Applied Optics*, **21**(9) (1982) 2558–62.